

A Generalized Gaussian Process Model for Computer Experiments with Binary Time Series

Chih-Li Sung^{a 1}, Ying Hung^{b 1}, William Rittase^c, Cheng Zhu^c,
 C. F. J. Wu^{a 2}

^aSchool of Industrial and Systems Engineering, Georgia Institute of Technology

^bDepartment of Statistics, Rutgers, the State University of New Jersey

^cDepartment of Biomedical Engineering, Georgia Institute of Technology

Abstract

Conventional analysis for computer experiments is based on Gaussian process (GP) models. Non-Gaussian observations such as binary responses are common in some computer experiments, but the extensions of GP models to these cases have received scant attention in the literature. Motivated by the analysis of a class of cell adhesion experiments, we introduce a generalized Gaussian process model for binary responses, which shares some common features with standard GP models. In addition, the proposed model incorporates a flexible mean function that can capture different types of time series structures. Asymptotic properties of the estimators are derived and their performance is examined via a simulation study. An optimal predictor and its predictive distribution are constructed based on the proposed model. The methodology is applied to study two different cell adhesion mechanisms, which were conducted by computer simulations. The fitted models reveal important biological differences between the two mechanisms in repeated bindings, which cannot be directly observed experimentally.

Keywords: Computer experiment, Gaussian process model, Single molecule experiment, Uncertainty quantification

¹Joint first authors.

²Corresponding author.

1 Introduction

Cell adhesion plays an important role in many physiological and pathological processes. This research is motivated by the analysis of a class of cell adhesion experiments called micropipette adhesion frequency assays, which is a method for measuring the kinetic rates between molecules in their native membrane environment. In a micropipette adhesion frequency assay, a red blood coated in a specific ligand is brought into contact with cell containing the native receptor for a predetermined duration, then retracted. The output of interest is binary, indicating whether a controlled contact results in adhesion. If there is an adhesion between molecules at the end of contact, retraction will stretch the red cell. If no adhesion resulted, the red cell will not be stretched. The kinetics of the molecular interaction can be derived through many repeated trials. In theory, these contacts should be independent Bernoulli trials. However, that there is a memory effect in the repeated tests and the quantification of such a memory effect is scientifically important (Zarnitsyna et al., 2007; Hung et al., 2008).

A cost-effective way to study the repeated adhesion frequency assays is through computer simulations, which study real systems using complex mathematical models and numerical tools like finite element analysis. They have been widely used as alternatives to physical experiments or observations, especially for the study of complex systems. In many such situations, a physical experiment or observation may be infeasible because it is unethical, impossible, inconvenient or too expensive. For cell adhesion in particular, performing physical experiments (i.e., lab work) is time-consuming and often involves complicated experimental manipulation. They are also prone to errors. Therefore, instead of performing the actual lab work, computer simulations of mathematical models provide an efficient way to examine the complex mechanisms behind the adhesion. Moreover, the analysis

based on computer simulations can provide insights on the biology that may not be directly obtainable in lab experiments. In the statistics literature, these simulations are also called computer experiments (Santner et al., 2003).

Computer experiments, while cheaper compared with physical experiments, can often have long run times. Typically they are deterministic in the sense that the same input produces the same output. Therefore, it is desirable to build an interpolator for the computer experiment outputs and use it as an “emulator” or “surrogate model” to predict results at untried input settings (Sacks et al., 1989; Santner et al., 2003). As a result, Gaussian process models whose predictors have the interpolation property are widely used as emulators for the analysis of computer experiments. Apart from the interpolation property, GP is popular for modeling complex systems because it can accommodate nonlinearity. The applications of GP can be found in many fields in science and engineering. Beyond deterministic simulations, GP-like models are also successful in applications to stochastic simulations by incorporating a nugget effect into the model (Santner et al. (2003), Section 4).

The conventional GP models are developed based on the Gaussian assumption, which does not hold in some scientific studies. For example, the focus of the cell adhesion frequency assays is to elicit the relationship between the setting of kinetic parameters/covariates and the adhesion score, which is binary. For binary outputs, the Gaussian assumption is not valid and GP models cannot be directly applied. Binary responses are common in computer experiments, but the extensions of GP models to non-Gaussian cases have received scant attention in the literature. Some studies such as in machine learning and spatial statistics (Rasmussen and Williams, 2006; Zhang, 2002) attempt to extend GP to non-Gaussian distributions. But the theoretical properties of estimators are not systematically studied. Moreover, an analogy to the GP predictive distribution for binary data is important for uncertainty quantification, but has not yet been developed to the best of our knowledge.

Apart from the non-Gaussian responses, analysis of the repeated cell adhesion frequency assays poses another challenge, namely, how to incorporate a time series structure with complex interaction effects. It was discovered that cells appear to have the ability to remember the previous adhesion events and such a memory has an impact on the future adhesion behaviors (Zarnitsyna et al., 2007; Hung et al., 2008). The quantification of the memory effect and how it interacts with the settings of the kinetic parameters in the binary time series are important but cannot be obtained by direct application of the conventional GP models. To consider the time series structure, a common practice is to construct a spatial-temporal model. However, a separable correlation function in which space and time are assumed to be independent is often implemented as a convenient way to address the computational issue. As a result, the estimation of interaction between space and time, which is of major interest here, is not allowed for. Therefore, a new model that can model binary time series and capture interaction effects is called for.

To overcome the aforementioned limitations, we introduce a new class of models in this article. The idea is to generalize GP models to non-Gaussian responses and incorporate a flexible mean function that can estimate the time series structure and its interaction with the input variables. In particular, we focus on binary responses and introduce a new model which is analogous to the GP model with an optimal interpolating predictor. Rigorous studies of estimation, prediction, and inference are required for the proposed model and the derivations are complicated by the nature of binary response and the dependency of time series.

The remainder of this article is organized as follows. The new class of models is discussed in Section 2. In Section 3, asymptotic properties of the estimators are derived and the predictive distributions are constructed. Finite sample performance is demonstrated by simulations in Section 4. In Section 5, the proposed method is illustrated with the analysis

of computer experiments for cell adhesion frequency assays. Concluding remarks are given in Section 6. An implementation for our method can be found in `binaryGP` (Sung, 2017) in `R` (R Core Team, 2015).

2 Model

2.1 Generalized Gaussian process models for binary time series

Suppose a computer experiment has a d -dimensional input setting $\mathbf{x} = (x_1, \dots, x_d)'$ and for each setting a sequence of *binary time series* output $\{y_t(\mathbf{x})\}_{t=1}^T$ is generated. In order to analyze these binary time series results from computer experiments, we introduce a generalized Gaussian process model based on the logit link function as follows:

$$\text{logit}(p_t(\mathbf{x})) = \eta_t(\mathbf{x}) = \sum_{r=1}^R \varphi_r y_{t-r}(\mathbf{x}) + \alpha_0 + \mathbf{x}'\boldsymbol{\alpha} + \sum_{l=1}^L \boldsymbol{\gamma}_l \mathbf{x} y_{t-l}(\mathbf{x}) + Z_t(\mathbf{x}), \quad (1)$$

where $p_t(\mathbf{x}) = \mathbb{E}[y_t(\mathbf{x})|H_t]$ is the conditional mean given the previous information $H_t = \{y_{t-1}(\mathbf{x}), y_{t-2}(\mathbf{x}), \dots\}$, and $Z_t(\cdot)$ is a Gaussian process with zero mean, variance σ^2 , and correlation function $R_{\boldsymbol{\theta}}(\cdot, \cdot)$ with unknown correlation parameters $\boldsymbol{\theta}$. Here Z_t is assumed to vary independently over time. In the computer experiment literature (Santner et al., 2003), the *power exponential correlation function* is commonly used and defined by

$$R_{\boldsymbol{\theta}}(\mathbf{x}_i, \mathbf{x}_j) = \exp \left\{ - \sum_{l=1}^d \frac{(x_{il} - x_{jl})^p}{\theta_l} \right\},$$

where $\boldsymbol{\theta} = (\theta_1, \dots, \theta_d)$, the power p controls the smoothness of the output surface, and the parameter θ_l controls the decay of correlation with respect to the distance between x_{il} and

x_{jl} . In model (1), $\{\varphi_r\}_{r=1}^R$ represents an autoregressive (AR) process with order R , and $\boldsymbol{\alpha} = (\alpha_1, \dots, \alpha_d)'$ represents the effects of \mathbf{x} , and $\{\boldsymbol{\gamma}_l\}_{l=1}^L$, where $\boldsymbol{\gamma}_l$ is a d -dimensional vector and represents the interaction between the input and the past outputs, which provides the flexibility of modeling different time series structures with different inputs.

This model includes several important models as special cases. When there is only one binary response for each input setting (i.e., $T = 1$), a special case of (1) can be written as

$$\text{logit}(p(\mathbf{x})) = \mu(\mathbf{x}) + Z(\mathbf{x}), \quad (2)$$

where the mean function is $\mu(\mathbf{x}) = \alpha_0 + \mathbf{x}'\boldsymbol{\alpha}$. This is a generalization of the GP model to binary data with logistic link. When \mathbf{x} is limited to the two-dimensional spatial domain, (2) becomes the spatial generalized linear mixed model (Zhang, 2002). On the other hand, if the interest is in modeling the autoregressive model, the first two terms on the right hand side of (1) form the Zeger-Qaqish (1988) model:

$$\text{logit}(p_t(\mathbf{x})) = \eta_t = \sum_{r=1}^R \varphi_r y_{t-r} + \alpha_0 + \mathbf{x}'\boldsymbol{\alpha}.$$

Model (1) extends the application of conventional GP to binary time series generated from computer experiments. The model is intuitively appealing; however, the issues of estimation, prediction, and inference are not straightforward due to the nature of binary response and the dependency of time series.

2.2 Estimation

Given n input settings $\mathbf{x}_1, \dots, \mathbf{x}_n$ in a computer experiment, denote $y_{it} \equiv y_t(\mathbf{x}_i)$ as the binary output generated from input \mathbf{x}_i at time t , where $\mathbf{x}_i \in \mathbb{R}^d$, $i = 1, \dots, n$, and $t = 1, \dots, T$.

Let N be the total number of the outputs, i.e., $N = nT$. In addition, at each time t , denote \mathbf{y}_t as an n -dimensional vector $\mathbf{y}_t = (y_{1t}, \dots, y_{nt})'$ with conditional mean $\mathbf{p}_t = (p_{1t}, \dots, p_{nt})'$, where $p_{it} = \mathbb{E}(y_{it}|H_{it})$ and $H_{it} = \{y_{i,t-1}, y_{i,t-2}, \dots\}$. Based on the data, model (1) can be rewritten into matrix form as follows:

$$\text{logit}(\mathbf{p}) = \mathbf{X}'\boldsymbol{\beta} + \mathbf{Z}, \quad \mathbf{Z} \sim \mathcal{N}(\mathbf{0}_N, \Sigma(\boldsymbol{\omega})), \quad (3)$$

where $\mathbf{p} = (\mathbf{p}'_1, \dots, \mathbf{p}'_T)'$, $\boldsymbol{\beta} = (\varphi_1, \dots, \varphi_R, \alpha_0, \boldsymbol{\alpha}', (\boldsymbol{\gamma}'_1, \dots, \boldsymbol{\gamma}'_L)')'$, $\boldsymbol{\omega} = (\sigma^2, \boldsymbol{\theta})'$, $\mathbf{Z} = (Z_1(\mathbf{x}_1), \dots, Z_1(\mathbf{x}_n), \dots, Z_T(\mathbf{x}_1), \dots, Z_T(\mathbf{x}_n))'$, \mathbf{X} is the model matrix $(X'_1, \dots, X'_T)'$, X_t is an $n \times (1 + R + d + dL)$ matrix with i -th row defined by $(X_t)_i = (1, y_{i,t-1}, \dots, y_{i,t-R}, \mathbf{x}'_i, \mathbf{x}'_i y_{i,t-1}, \dots, \mathbf{x}'_i y_{i,t-L})$, and $\Sigma(\boldsymbol{\omega})$ is an $N \times N$ covariance matrix defined by

$$\Sigma(\boldsymbol{\omega}) = \sigma^2 \mathbf{R}_{\boldsymbol{\theta}} \otimes I_T \quad (4)$$

with $(\mathbf{R}_{\boldsymbol{\theta}})_{ij} = R_{\boldsymbol{\theta}}(\mathbf{x}_i, \mathbf{x}_j)$.

With the presence of time series and their interaction with the input settings in model (1), we can write down the partial likelihood (PL) function (Cox, 1972, 1975) according to the formulation of Slud and Kedem (1994). Given the previous information $\{H_{it}\}_{i=1, \dots, n; t=1, \dots, N}$, the PL for $\boldsymbol{\beta}$ can be written as

$$PL(\boldsymbol{\beta}|\mathbf{Z}) = \prod_{i=1}^n \prod_{t=1}^T (p_{it}(\boldsymbol{\beta}|\mathbf{Z}))^{y_{it}} (1 - p_{it}(\boldsymbol{\beta}|\mathbf{Z}))^{1-y_{it}},$$

where $p_{it}(\boldsymbol{\beta}|\mathbf{Z}) = \mathbb{E}_{\boldsymbol{\beta}|\mathbf{Z}}[y_{it}|H_{it}]$. Then, the integrated quasi-PL function for the estimation of $(\boldsymbol{\beta}, \boldsymbol{\omega})$ is given by

$$|\Sigma(\boldsymbol{\omega})|^{-1/2} \int \exp\{\log PL(\boldsymbol{\beta}|\mathbf{Z}) - \frac{1}{2} \mathbf{Z}' \Sigma(\boldsymbol{\omega})^{-1} \mathbf{Z}\} d\mathbf{Z}.$$

Because of the difficulty in computing the integrated quasi-PL function, a *penalized quasi-PL* (PQPL) function is used as an approximation. Similar to the procedure in Breslow and Clayton (1993), the integrated quasi-partial log-likelihood can be approximated by Laplace's method (Barndorff-Nielsen and Cox, 1997). Ignoring the multiplicative constant and plugging (4) in $\Sigma(\boldsymbol{\omega})$, the approximation yields

$$-\frac{1}{2} \log |I_n + \sigma^2 \mathbf{W}(\mathbf{R}_\theta \otimes I_T)| + \sum_{i=1}^n \sum_{t=1}^T \left(y_{it} \log \frac{p_{it}(\boldsymbol{\beta}|\tilde{\mathbf{Z}})}{1 - p_{it}(\boldsymbol{\beta}|\tilde{\mathbf{Z}})} + \log(1 - p_{it}(\boldsymbol{\beta}|\tilde{\mathbf{Z}})) \right) - \frac{1}{2\sigma^2} \tilde{\mathbf{Z}}' (\mathbf{R}_\theta \otimes I_T)^{-1} \tilde{\mathbf{Z}}, \quad (5)$$

where \mathbf{W} is an $N \times N$ diagonal matrix with diagonal elements $W_{it} = p_{it}(\boldsymbol{\beta}|\tilde{\mathbf{Z}})(1 - p_{it}(\boldsymbol{\beta}|\tilde{\mathbf{Z}}))$, $p_{it}(\boldsymbol{\beta}|\tilde{\mathbf{Z}}) = \mathbb{E}_{\boldsymbol{\beta}|\tilde{\mathbf{Z}}}[y_{it}|H_{it}]$, and $\tilde{\mathbf{Z}} = \tilde{\mathbf{Z}}(\boldsymbol{\beta}, \boldsymbol{\omega})$ is the solution of $\sum_{i=1}^n \sum_{t=1}^T \mathbf{e}_{it}(y_{it} - p_{it}(\boldsymbol{\beta}|\tilde{\mathbf{Z}})) = (\mathbf{R}_\theta \otimes I_T)^{-1} \mathbf{Z}/\sigma^2$, where \mathbf{e}_{it} is a unit-vector where $((t-1)n+i)$ -th element is one. Thus, similar to the derivations in Breslow and Clayton (1993) for score equations of a penalized quasi-likelihood function, the score equations of the PQPL function for $\boldsymbol{\beta}$ and $\boldsymbol{\omega}$ are

$$\sum_{i=1}^n \sum_{t=1}^T X_{it}(y_{it} - p_{it}(\boldsymbol{\beta}, \boldsymbol{\omega})) = 0$$

and

$$\sum_{i=1}^n \sum_{t=1}^T \mathbf{e}_{it}(y_{it} - p_{it}(\boldsymbol{\beta}, \boldsymbol{\omega})) = (\mathbf{R}_\theta \otimes I_T)^{-1} \mathbf{Z}/\sigma^2,$$

where $p_{it}(\boldsymbol{\beta}, \boldsymbol{\omega}) = \mathbb{E}_{\boldsymbol{\beta}, \boldsymbol{\omega}}[y_{it}|H_{it}]$. The solution to this score equations can be efficiently obtained by an iterated weighted least squares (IWLS) approach as follows. In each step, one first solves

$$(\mathbf{X}' \mathbf{V}(\boldsymbol{\omega})^{-1} \mathbf{X}) \boldsymbol{\beta} = \mathbf{X}' \mathbf{V}(\boldsymbol{\omega})^{-1} \tilde{\boldsymbol{\eta}}, \quad (6)$$

where $\mathbf{V}(\boldsymbol{\omega}) = \mathbf{W}^{-1} + \sigma^2(\mathbf{R}_{\boldsymbol{\theta}} \otimes I_T)$, $\tilde{\eta}_{it} = \log \frac{p_{it}(\boldsymbol{\beta}, \boldsymbol{\omega})}{1-p_{it}(\boldsymbol{\beta}, \boldsymbol{\omega})} + \frac{y_{it} - p_{it}(\boldsymbol{\beta}, \boldsymbol{\omega})}{p_{it}(\boldsymbol{\beta}, \boldsymbol{\omega})(1-p_{it}(\boldsymbol{\beta}, \boldsymbol{\omega}))}$, and then sets

$$\hat{\mathbf{Z}} = (\mathbf{R}_{\boldsymbol{\theta}} \otimes I_T) \mathbf{V}(\boldsymbol{\omega})^{-1} (\tilde{\boldsymbol{\eta}} - \mathbf{X}' \hat{\boldsymbol{\beta}}) / \sigma^2. \quad (7)$$

Estimation of the correlation parameters $\boldsymbol{\theta}$ and variance σ^2 is obtained by the restricted maximum likelihood (REML) approach (Patterson and Thompson, 1971) because it is known to have smaller bias comparing with the maximum likelihood approach (Patterson and Thompson, 1974). According to Harville (1974, 1977), the REML estimators of σ^2 and $\boldsymbol{\theta}$ can be solved by minimizing the following negative log-likelihood function with respect to $\boldsymbol{\omega}$,

$$L(\boldsymbol{\omega}) = \frac{N-m}{2} \log(2\pi) - \frac{1}{2} \log(|\mathbf{X}' \mathbf{X}|) + \frac{1}{2} \log(|\mathbf{V}(\boldsymbol{\omega})|) + \frac{1}{2} \log(|\mathbf{X}' \mathbf{V}(\boldsymbol{\omega})^{-1} \mathbf{X}|) + \frac{1}{2} \tilde{\boldsymbol{\eta}}' \Pi(\boldsymbol{\omega}) \tilde{\boldsymbol{\eta}}, \quad (8)$$

where $m = 1 + R + d + dL$ and $\Pi(\boldsymbol{\omega}) = \mathbf{V}(\boldsymbol{\omega})^{-1} - \mathbf{V}(\boldsymbol{\omega})^{-1} \mathbf{X} (\mathbf{X}' \mathbf{V}(\boldsymbol{\omega})^{-1} \mathbf{X})^{-1} \mathbf{X}' \mathbf{V}(\boldsymbol{\omega})^{-1}$.

Therefore, the estimators $\hat{\boldsymbol{\beta}}$ and $\hat{\boldsymbol{\omega}}$ ($\equiv (\hat{\sigma}^2, \hat{\boldsymbol{\theta}})'$) can be obtained by iteratively solving (6), (7) and minimizing (8). Note that $\mathbf{V}(\boldsymbol{\omega})$ is a block diagonal matrix, i.e., a square matrix having main diagonal blocks square matrices such that the off-diagonal blocks are zero matrices. Therefore the computational burden for the matrix inversion of $\mathbf{V}(\boldsymbol{\omega})$ can be alleviated by the fact that the inverse of a block diagonal matrix is a block diagonal matrix, composed of the inversion of each block.

2.3 Asymptotic Properties

Asymptotic results are presented here to show that the estimators $\hat{\boldsymbol{\beta}}$, $\hat{\sigma}^2$ and $\hat{\boldsymbol{\theta}}$ obtained in Section 2.2 are asymptotically normally distributed. The assumptions are given in Appendix A, and the proofs are stated in Appendices B and C. These results are developed along the

lines described in Hung et al. (2008) and Cressie and Lahiri (1993, 1996).

Theorem 2.1. *Under assumptions A1 and A2, the maximum quasi-PL estimator for the fixed effects β are consistent and asymptotically normal as $N \rightarrow \infty$,*

$$\sqrt{N}(\hat{\beta} - \beta) = \Lambda_N^{-1} \frac{1}{\sqrt{N}} S_N(\beta, \omega) + o_p(1)$$

and

$$\sqrt{N} \Lambda_N^{1/2}(\hat{\beta} - \beta) \xrightarrow{d} \mathcal{N}(\mathbf{0}, I_m),$$

where m is the size of the vector β (i.e., $m = 1 + R + d + dL$), the sample information matrix

$$\Lambda_N = \frac{1}{N} \sum_{i=1}^n \sum_{t=1}^T X_{it} X'_{it} p_{it}(\beta, \omega) (1 - p_{it}(\beta, \omega)),$$

and $S_n(\beta, \omega) = \sum_{i=1}^n \sum_{t=1}^T X_{it} (y_{it} - p_{it}(\beta, \omega))$.

Theorem 2.2. *Denote $[\Gamma_N(\omega)]_{i,j} = \partial^2 L(\omega) / \partial \omega_i \partial \omega_j$ and $J_N(\omega) = [\mathbb{E}_\omega \Gamma_N(\omega)]^{1/2}$. Then, under assumptions A3 and A4,*

$$J_N(\hat{\omega})(\hat{\omega} - \omega) \xrightarrow{d} \mathcal{N}(\mathbf{0}, I_{d+1}).$$

3 Construction of Predictive Distribution

For computer experiments, the construction of an optimal predictor and its corresponding predictive distribution is important for uncertainty quantification, sensitivity analysis, process optimization, and calibration (Santner et al., 2003). Note that, for simplicity, the results in this section are based on the assumption that the parameters are known. When the parameters are estimated as described in Section 2, the plugin approaches can be easily

implemented (Santner et al., 2003). For some untried setting \mathbf{x}_{n+1} , denote the predictive probability at time s by $p_s(\mathbf{x}_{n+1}) = \mathbb{E}[y_s(\mathbf{x}_{n+1})]$. We first present the following lemma which lays the foundation for the construction of predictive distribution. Assume that $D_{n+1,s}$ includes the “previous information” $\{y_{n+1,s-1}, y_{n+1,s-2}, \dots, p_{n+1,s-1}, p_{n+1,s-2}, \dots\}$ at \mathbf{x}_{n+1} and $\{y_{it}, p_{it}\}$, where $i = 1, \dots, n$ and $t = 1, \dots, T$. Given $D_{n+1,s}$, the following result shows that the conditional distribution of $p_s(\mathbf{x}_{n+1})$ is logit-normal. The proof is given in Appendix D.

Lemma 3.1. *The conditional distribution of $p_s(\mathbf{x}_{n+1})$ can be written as*

$$p_s(\mathbf{x}_{n+1})|D_{n+1,s} \sim \text{Logitnormal}(m(D_{n+1,s}), v(D_{n+1,s})),$$

where

$$m(D_{n+1,s}) = \sum_{r=1}^R \varphi_r y_{n+1,s-r} + \mathbf{x}'_{n+1} \boldsymbol{\alpha} + \sum_{l=1}^L \boldsymbol{\gamma}_l \mathbf{x}_{n+1} y_{n+1,s-l} + \mathbf{r}'_{\boldsymbol{\theta}} \mathbf{R}_{\boldsymbol{\theta}}^{-1} \left(\log \frac{\mathbf{p}_s}{\mathbf{1}_n - \mathbf{p}_s} - \boldsymbol{\mu}_s \right),$$

$$v(D_{n+1,s}) = \sigma^2 (1 - \mathbf{r}'_{\boldsymbol{\theta}} \mathbf{R}_{\boldsymbol{\theta}}^{-1} \mathbf{r}_{\boldsymbol{\theta}}), \quad \mathbf{r}_{\boldsymbol{\theta}} = (R_{\boldsymbol{\theta}}(\mathbf{x}_{n+1}, \mathbf{x}_1), \dots, R_{\boldsymbol{\theta}}(\mathbf{x}_{n+1}, \mathbf{x}_n))', \quad \mathbf{R}_{\boldsymbol{\theta}} = \{R_{\boldsymbol{\theta}}(\mathbf{x}_i, \mathbf{x}_j)\},$$

$$\mathbf{p}_s = (p_s(\mathbf{x}_1), \dots, p_s(\mathbf{x}_n))', \text{ and } (\boldsymbol{\mu}_s)_i = \sum_{r=1}^R \varphi_r y_{i,s-r} + \mathbf{x}'_i \boldsymbol{\alpha} + \sum_{l=1}^L \boldsymbol{\gamma}_l \mathbf{x}_i y_{i,s-l}.$$

Note that $\text{Logitnormal}(\mu, \sigma^2)$ represents a logit-normal distribution P , where $P = \exp\{X\}/(1 + \exp\{X\})$ and X has a univariate normal distribution with μ and variance σ^2 . Denote the first two moments of the distribution by $\mathbb{E}[P] = \kappa(\mu, \sigma^2)$ and $\mathbb{V}[P] = \tau(\mu, \sigma^2)$. In general, there is no closed form expression for $\kappa(\mu, \sigma^2)$ and $\tau(\mu, \sigma^2)$, but it can be easily computed by numerical integration such as in the package `logitnorm` (Wutzler, 2012) in `R` (R Core Team, 2015). More discussions on *logit-normal distribution* can be found in Mead (1965); Atchison and Shen (1980); Frederic and Lad (2008).

Based on the Lemma, the prediction of $p_s(\mathbf{x}_{n+1})$ for some untried setting \mathbf{x}_{n+1} and its

variance can then be obtained in the next theorem. The proof is given in Appendix E.

Theorem 3.2. *Given $D_{n+1,s} = \{\mathbf{y}'_1, \dots, \mathbf{y}'_T, \mathbf{p}'_1, \dots, \mathbf{p}'_T, y_{n+1,s-1}, \dots, y_{n+1,1}, p_{n+1,s-1}, \dots, p_{n+1,1}\}$,*

(i) the minimum mean squared error (MMSE) predictor of $p_s(\mathbf{x}_{n+1})$ is

$$\mathbb{E}[p_s(\mathbf{x}_{n+1})|D_{n+1,s}] = \kappa(m(D_{n+1,s}), v(D_{n+1,s}))$$

with variance $\mathbb{V}[p_s(\mathbf{x}_{n+1})|D_{n+1,s}] = \tau(m(D_{n+1,s}), v(D_{n+1,s}))$;

(ii) the MMSE predictor is an interpolator, i.e., if $\mathbf{x}_{n+1} = \mathbf{x}_i$ for $i = 1, \dots, n$, then

$$\mathbb{E}[p_s(\mathbf{x}_{n+1})|D_{n+1,s}] = p_s(\mathbf{x}_i) \text{ and } \mathbb{V}[p_s(\mathbf{x}_{n+1})|D_{n+1,s}] = 0;$$

(iii) the q -th quantile of the conditional distribution $p(\mathbf{x}_{n+1})|D_{n+1,s}$ is

$$\frac{\exp\{m(D_{n+1,s}) + z_q \sqrt{v(D_{n+1,s})}\}}{1 + \exp\{m(D_{n+1,s}) + z_q \sqrt{v(D_{n+1,s})}\}},$$

where z_q is the q -th quantile of the standard normal distribution.

This result can be used for prediction and quantification of the predictive uncertainty, such as constructing the predictive confidence interval for some untried settings at any confidence level.

Based on Theorem 3.2, the MMSE predictor of $p_s(\mathbf{x}_{n+1})$ given \mathbf{Y} , including $\mathbf{y}'_1, \dots, \mathbf{y}'_T$, and $y_1(\mathbf{x}_{n+1}), \dots, y_{s-1}(\mathbf{x}_{n+1})$, can be obtained in the following corollary.

Corollary 3.3. *Let $\mathbf{p} = (\mathbf{p}'_1, \dots, \mathbf{p}'_T, p_1(\mathbf{x}_{n+1}), \dots, p_{s-1}(\mathbf{x}_{n+1}))'$. Then, given $\mathbf{Y} = (\mathbf{y}'_1, \dots, \mathbf{y}'_T, y_1(\mathbf{x}_{n+1}), \dots, y_{s-1}(\mathbf{x}_{n+1}))'$, the minimum mean squared error (MMSE) predictor of $p_s(\mathbf{x}_{n+1})$ is*

$$\mathbb{E}[p_s(\mathbf{x}_{n+1})|\mathbf{Y}] = \mathbb{E}_{\mathbf{p}|\mathbf{Y}}[\kappa(m(D_{n+1,s}), v(D_{n+1,s}))|\mathbf{Y}]$$

with variance

$$\mathbb{V}[p_s(\mathbf{x}_{n+1})|\mathbf{Y}] = \mathbb{E}_{\mathbf{p}|\mathbf{Y}}[\tau(m(D_{n+1,s}), v(D_{n+1,s}))|\mathbf{Y}] + \mathbb{V}_{\mathbf{p}|\mathbf{Y}}[\kappa(m(D_{n+1,s}), v(D_{n+1,s}))|\mathbf{Y}].$$

Although the distribution $\mathbf{p}|\mathbf{Y}$ cannot provide a closed form, the random samples from $\mathbf{p}|\mathbf{Y}$ can be generated through the Metropolis-Hastings (MH) algorithm. Thus, based on these samples, the expectation and variance in Corollary 3.3 can be approximated by using a Monte Carlo method. For example, let $\{\mathbf{p}^{(j)}\}_{j=1,\dots,J}$ be the J random samples generated from distribution $\mathbf{p}|\mathbf{Y}$, then the MMSE predictor of $p_s(\mathbf{x}_{n+1})$ in Corollary 3.3 can be approximated by

$$\mathbb{E}_{\mathbf{p}|\mathbf{Y}}[\kappa(m(D_{n+1,s}), v(D_{n+1,s}))|\mathbf{Y}] \approx \frac{1}{J} \sum_{j=1}^J \kappa(m(D_{n+1,s}^{(j)}), v(D_{n+1,s}^{(j)})),$$

where $D_{n+1,s}^{(j)} = \{\mathbf{p}^{(j)}, \mathbf{Y}\}$. The explicit MH algorithm is given in Appendix F. Note that in the MH algorithm, we first sample a value for the k -th component p_k from the conditional distribution of p_k given $p_j, y_j, j \neq k$, which is $\text{Logitnormal}(m(\mathbf{p}_{-k}, \mathbf{y}_{-k}), v(\mathbf{p}_{-k}, \mathbf{y}_{-k}))$, where

$$m(\mathbf{p}_{-k}, \mathbf{y}_{-k}) = \mu_t(\mathbf{x}_i) - \sum_{k \neq j} \frac{Q_{kj}}{Q_{kk}} \left(\log \frac{p_k}{1 - p_k} - \mu_t(\mathbf{x}_i) \right), \quad v(\mathbf{p}_{-k}, \mathbf{y}_{-k}) = \frac{\sigma^2}{Q_{kk}},$$

in which $\mu_t(\mathbf{x}_i) = \sum_{r=1}^R \varphi_r y_{i,t-r} + \mathbf{x}'_i \boldsymbol{\alpha} + \sum_{l=1}^L \gamma_l \mathbf{x}_i y_{i,t-l}$ and Q_{kj} is the (k, j) -element of $\mathbf{R}_{\boldsymbol{\theta}}^{-1}$. Similar to Zhang (2002), we use the single-component MH algorithm, that is, to update only a single component at each iteration. Moreover, the proposed distribution $f(p_k)$ is used for the single MH algorithm, so that the probability of accepting a new p_k^* is the minimum of 1 and $\frac{f(p_k^*|y_k)f(p_k)}{f(p_k|y_k)f(p_k^*)} \left(= \frac{f(y_k|p_k^*)}{f(y_k|p_k)} \right)$.

Although the previous time series for an untried setting in Corollary 3.3 (i.e., $y_1(\mathbf{x}_{n+1}), \dots,$

$y_{s-1}(\mathbf{x}_{n+1})$) is typically unknown in practice, we can emulate a completely new time series (or batch of time series) with input \mathbf{x}_{n+1} . The idea is to generate draws from the conditional distribution $p_s(\mathbf{x}_{n+1})|\mathbf{Y}$ for future outputs, starting from $s = 0$, and take pointwise median of the random draws. This idea is similar to the dynamic emulators introduced by Liu and West (2009) for continuous outputs. The random samples from $p_s(\mathbf{x}_{n+1})|\mathbf{Y}$ can be generated by the fact $f(p_s(\mathbf{x}_{n+1}), \mathbf{p}|\mathbf{Y}) = f(\mathbf{p}|\mathbf{Y})f(p_s(\mathbf{x}_{n+1})|\mathbf{p}, \mathbf{Y})$, where $f(p_s(\mathbf{x}_{n+1})|\mathbf{p}, \mathbf{Y})$ is a logit-normal distribution provided in Lemma 3.1. As mentioned above, the random samples from $f(\mathbf{p}|\mathbf{Y})$ can be generated through the MH algorithm. Therefore, generating a draw from $p_s(\mathbf{x}_{n+1})|\mathbf{Y}$ consists of two steps: (1) generating the “previous” probability values \mathbf{p}^* given output \mathbf{Y} from the distribution $\mathbf{p}|\mathbf{Y}$ through the MH algorithm, and (2) based on the sample \mathbf{p}^* , draw a sample $p_s^*(\mathbf{x}_{n+1})$ from $p_s(\mathbf{x}_{n+1})|\mathbf{p}^*, \mathbf{Y}$, which is a logit-normal distribution, and also draw a sample $y_s^*(\mathbf{x}_{n+1})$ from a Bernoulli distribution with parameter $p_s^*(\mathbf{x}_{n+1})$. An explicit algorithm is given in Appendix G.

4 Simulation Studies

Simulation studies are conducted in this section to demonstrate the performance of the proposed model in terms of estimation and prediction. Furthermore, we also implement the proposed approaches to quantify the prediction uncertainty in some simulation examples. Consider $d = 5$, $\alpha_0 = 0.5$, $\boldsymbol{\alpha} = (-3, 2, -2, 1, 0.5)'$, $\sigma^2 = 1$, $\boldsymbol{\theta} = (0.5, 1.0, 1.5, 2.0, 2.5)'$, and $\varphi_1 = 0.8$. The input \mathbf{x} is randomly generated from a regular grid on $[0, 1]^5$ and the corresponding binary output $y_t(\mathbf{x})$ at time t is generated by a Bernoulli distribution with probability $p_t(\mathbf{x})$ calculated by (1). Four combinations of n and T are considered in the simulations.

The estimation results are reported in Table 1 based on 100 replicates for each sample

size combination. Based on Table 1(a), the proposed approach can estimate the parameters $(\alpha_0, \boldsymbol{\alpha}, \varphi_1)$ in the linear function with high accuracy. For the correlation parameters $\boldsymbol{\theta}$, the proposed approach tends to overestimate the correlation parameters for small sample size. This is not surprising because the estimation of correlation parameters is more challenging and the same phenomenon is observed in conventional GP models (see Li and Sudjianto (2005)). This problem can be ameliorated by the increase of sample size as shown in Table 1(b). Given the same number of total sample size, $(n = 200, T = 50)$ and $(n = 500, T = 20)$, it appears that a larger n can improve the estimation accuracy more effectively.

Based on the construction of predictive distribution in Section 3, we can emulate a completely new time series with an untried input. Here we generate 100 random untried inputs to examine its prediction performance. The prediction performance is evaluated by the following two measures. Define the 100 random untried inputs ($n_{\text{test}} = 100$) as $\mathbf{x}_1^*, \dots, \mathbf{x}_{100}^*$, the root mean squared prediction error is calculated by

$$\text{RMSPE} = \frac{1}{n_{\text{test}} T} \sum_{i=1}^{n_{\text{test}}} \sum_{t=1}^T (p_t(\mathbf{x}_i^*) - \hat{p}_t(\mathbf{x}_i^*))^2$$

and its misclassification rate (MR) is calculated by

$$\frac{1}{n_{\text{test}} T} \sum_{i=1}^{n_{\text{test}}} \sum_{t=1}^T (y_t(\mathbf{x}_i^*) - \hat{y}_t(\mathbf{x}_i^*))^2.$$

The RMSPE and MR results are given in Table 2. Overall, the proposed predictor has the root mean squared prediction error less than 0.12 and the misclassification rate less than 17.3%. Also, with the increase of sample size, the prediction error, in terms of both RMSPE and MR, decreases in general.

Furthermore, the predictive distributions can be used to quantify the prediction uncer-

n	T	$\hat{\alpha}_0$	$\hat{\alpha}_1$	$\hat{\alpha}_2$	$\hat{\alpha}_3$	$\hat{\alpha}_4$	$\hat{\alpha}_5$	$\hat{\varphi}_1$
200	20	0.4592 (0.1053)	-2.7148 (0.1503)	1.8182 (0.1334)	-1.8171 (0.1213)	0.9099 (0.0932)	0.4518 (0.1034)	0.7200 (0.1072)
200	50	0.4530 (0.0737)	-2.6810 (0.0965)	1.7972 (0.0882)	-1.7942 (0.0840)	0.8952 (0.0716)	0.4608 (0.0586)	0.7046 (0.0711)
500	20	0.4649 (0.0896)	-2.7574 (0.1382)	1.8200 (0.1174)	-1.8289 (0.1026)	0.9134 (0.0831)	0.4758 (0.0742)	0.7318 (0.0727)
500	50	0.4498 (0.0633)	-2.7491 (0.0740)	1.8323 (0.0566)	-1.8340 (0.0612)	0.9188 (0.0563)	0.4514 (0.0515)	0.7407 (0.0434)

(a) *Estimation of linear function coefficients.* The parameter settings are $\alpha_0 = 0.5, \alpha_1 = -3, \alpha_2 = 2, \alpha_3 = -2, \alpha_4 = 1, \alpha_5 = 0.5$, and $\varphi_1 = 0.8$.

n	T	$\hat{\theta}_1$	$\hat{\theta}_2$	$\hat{\theta}_3$	$\hat{\theta}_4$	$\hat{\theta}_5$	$\hat{\sigma}^2$
200	20	0.8627 (0.8093)	1.8039 (1.1289)	2.348 (1.4083)	3.2977 (1.7624)	4.1036 (1.8460)	0.8183 (0.0683)
200	50	0.6529 (0.1588)	1.5472 (0.6297)	2.3761 (1.1175)	3.0112 (1.2486)	3.8006 (1.4879)	0.7931 (0.0462)
500	20	0.6064 (0.1565)	1.1719 (0.2531)	1.9282 (0.5452)	2.6568 (0.9598)	3.2411 (1.1655)	0.8657 (0.0478)
500	50	0.5658 (0.0829)	1.1631 (0.1620)	1.7803 (0.3452)	2.3703 (0.3900)	3.1084 (0.6844)	0.8727 (0.0317)

(b) *Estimation of correlation parameters and variance.* The parameter settings are $\theta_1 = 0.5, \theta_2 = 1.0, \theta_3 = 1.5, \theta_4 = 2, \theta_5 = 2.5$, and $\sigma^2 = 1$.

Table 1: Simulation studies of parameter estimates.

tainty. The predictive distributions with two random untried inputs are shown in Figure 1, where the green dotted lines represent the true probability, the red dashed lines represent the MMSE predictors obtained in Corollary 3.3. From Figure 1, it appears that the MMSE predictors provide accurate predictions in both cases. Moreover, the predictive distributions

	$n = 200$ $T = 20$	$n = 200$ $T = 50$	$n = 500$ $T = 20$	$n = 500$ $T = 50$
RMSPE	0.1188 (0.66)	0.1193 (0.58)	0.1058 (0.60)	0.1053 (0.45)
MR (%)	17.22 (1.55)	17.27 (1.39)	17.08 (1.58)	16.83 (1.19)

Table 2: Comparison of RMSPEs and the misclassification rates.

provide rich information for statistical inference. For example, we can construct 95% predictive confidence intervals for the two untried settings as indicated in blue in Figure 1.

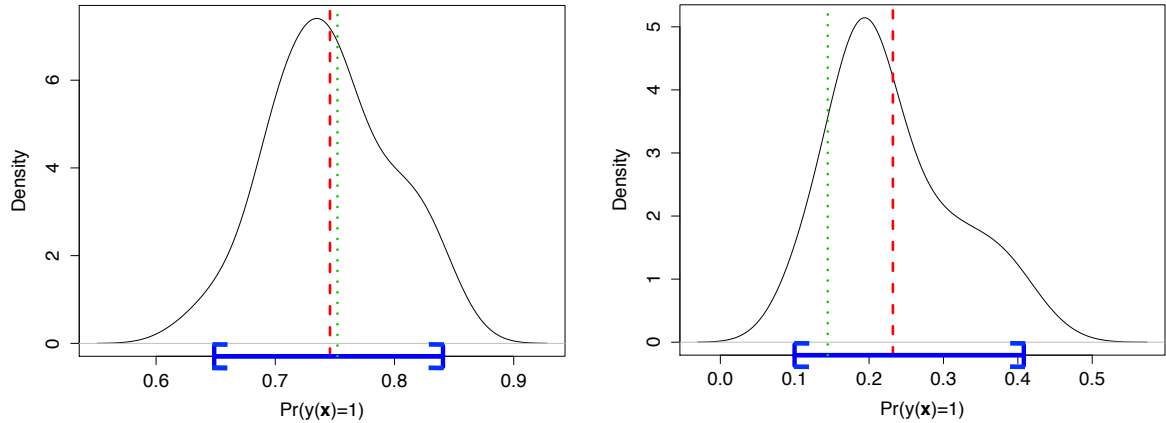


Figure 1: Predictive distributions. The green dotted lines are the true probability, the red dashed lines are the MMSE predictors, and the 95% predictive confidence intervals are indicated in blue.

5 Computer Experiments for Cell Adhesion Frequency Assay

In an earlier study based on *in vitro* experiments, an important memory effect was discovered in the repeated adhesion experiments of the micropipette adhesion frequency assay. However, only limited variables of interest can be studied in the lab because of the technical complexity of the biological setting and the complicated experimental manipulation. Therefore, computer simulation experiments are performed to examine the complex mechanisms behind repeated receptor-ligand binding to rigorously elucidate the biological mechanisms behind the memory effect.

In these computer experiments, two surfaces are simulated to reflect the two opposing membranes in the adhesion frequency assays. The molecules on the surfaces are permitted to interact for the contact duration and then separated for a period of waiting time to simulate the retract-approach phase of the assays. The computer experiments are constructed based on a kinetic proofreading model for receptor modification or other induced mechanisms (to be described later) and solved through a Gillespie algorithm. The contact is scored as 1 or 0 depending on whether at least one bond or no bond is observed, respectively. The process is repeated until the given number of contacts is completed.

The biological system investigated here is the T Cell Receptor (TCR) binding to antigen peptide bound to Major Histocompatibility Complex (pMHC), which has previously been shown to exhibit memory in repeated contacts (Zarnitsyna et al., 2007). The TCR is the primary molecule involved in detecting foreign antigens which are presented on pMHC molecules expressed by infected cells. Memory in serial interactions of these foreign antigens may be a mechanism which underlies the major properties of T cell antigen recognition: sensitivity, specificity, and context discrimination. It has largely remained uninvestigated

due to the small time scales at which the mechanism operates and the complexity of the experimental system. Although there are many possible cellular mechanisms which may induce this behavior, two specific mechanisms are proposed and investigated in this study as to how this memory may be controlled: 1) pMHC binding to a single TCR within a cluster upregulates the kinetics of all TCRs within that cluster (Figure 2 panel A), or 2) pulling by engaged pMHC of a single TCR within a cluster induces upregulated kinetics to the cluster of TCRs (Figure 2 panel B). The two mechanisms are called free induction mechanism and forced induction mechanism for brevity. The difference between the two is that the free induction mechanism only considers bonds that are spontaneously dissociated during the contact period before retraction pulls the two cells apart, hence would not have experienced any force, whereas the forced-induction mechanism only considers bonds that are forced to dissociate during retraction, hence would have experienced pulling force (Huang et al., 2010).

The free induction mechanism has six control variables given in Table 3. The range of each control variable in Table 3 is given by physical principles or estimated through similar molecular interactions. The design of the control variables is a 60-run OA-based Latin hypercube designs (Tang, 1993). For each run, it consists of 50 replicates and each replicate has 100 repeated contacts ($T = 100$).

Variable	Description	Range
$x_{K_{f,p}}$	on-rate enhancement of activated TCRs	(1,100)
$x_{K_{r,p}}$	off-rate enhancement of activated TCRs	(0.1,100)
$x_{T_{half}}$	half-life of cluster activation	(0.1,10)
x_{T_c}	cell-cell contact time	(0.1,10)
x_{T_w}	waiting time in between contacts	(0.1,10)
x_{K_c}	kinetic proofreading modification rate for activation of cluster	(0.1,10)

Table 3: *Control variables in cell adhesion frequency assay experiments.*

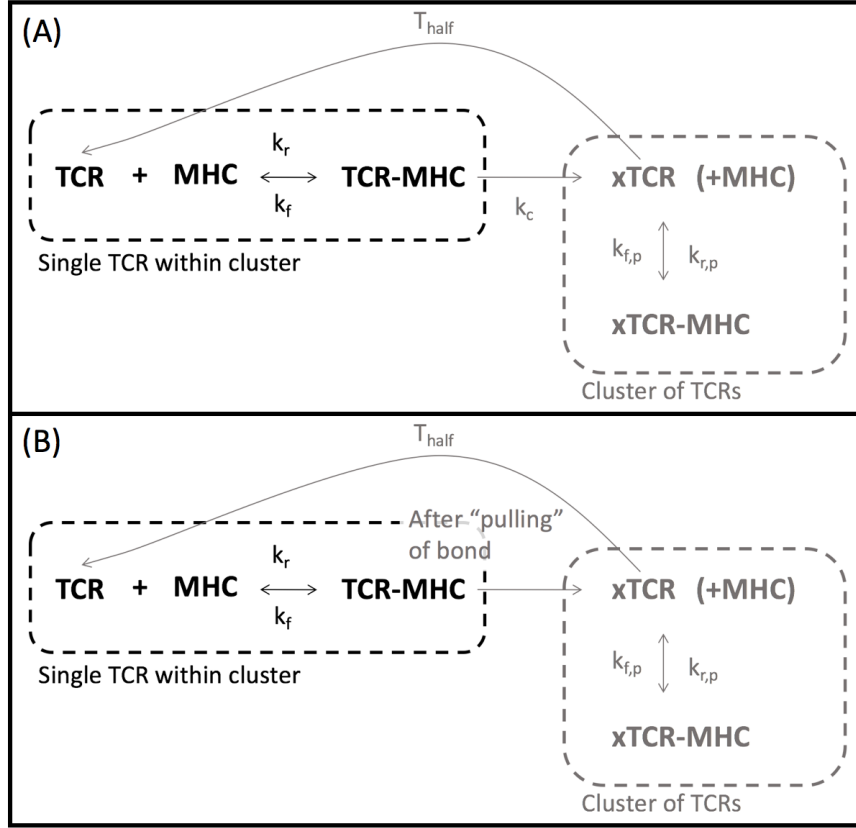


Figure 2: Two cellular mechanisms investigated in the study: (A) free induction mechanism and (B) forced induction mechanism.

To implement the proposed method, we can start with a larger model in which the mean function of model (1) includes all the main effects of the control variables and their interactions with the past time series outputs y_{t-r} and then identify significant effects based on the asymptotic results presented in Section 2.3. To save space, we demonstrate the procedure by a mean function that has all the main effects and their interaction terms with

y_{t-1} . The model is written as:

$$\text{logit}(p_t(\mathbf{x})) = -1.1175 + \hat{\varphi}_1 y_{t-1}(\mathbf{x}) + \hat{\alpha}_1 x_{K_{f,p}} + \hat{\alpha}_2 x_{K_{r,p}} + \hat{\alpha}_3 x_{T_{half}} + \hat{\alpha}_4 x_{Tc} + \hat{\alpha}_5 x_{Tw} + \hat{\alpha}_6 x_{Kc} + (\hat{\gamma}_1 x_{K_{f,p}} + \hat{\gamma}_2 x_{K_{r,p}} + \hat{\gamma}_3 x_{T_{half}} + \hat{\gamma}_4 x_{Tc} + \hat{\gamma}_5 x_{Tw} + \hat{\gamma}_6 x_{Kc}) y_{t-1}(\mathbf{x}) + Z_t(\mathbf{x}),$$

where all the control variables are standardized into $[0, 1]$, $\hat{\sigma} = 0.40$, the estimated power exponential (with $p = 2$) correlation parameters are $\hat{\boldsymbol{\theta}} = (\hat{\theta}_{K_{f,p}}, \hat{\theta}_{K_{r,p}}, \hat{\theta}_{T_{half}}, \hat{\theta}_{Tc}, \hat{\theta}_{Tw}, \hat{\theta}_{Kc}) = (2.2280, 0.3087, 1.8877, 0.0202, 2.2843, 0.0205)$, and the estimation and inference results for the mean function coefficients are given in Table 4. According to Table 4, $x_{T_{half}}$ has no significant effect in the mean function at the 0.01 level. By removing $x_{T_{half}}$, the model can be updated as

$$\begin{aligned} \text{logit}(p_t(\mathbf{x})) = & \\ & -1.1040 - 0.5872 y_{t-1}(\mathbf{x}) + 0.2348 x_{K_{f,p}} + 0.7134 x_{K_{r,p}} + 0.9825 x_{Tc} - 0.1452 x_{Tw} + 0.2466 x_{Kc} \\ & + (0.3130 x_{K_{f,p}} + 0.4745 x_{K_{r,p}} - 0.1610 x_{T_{half}} + 0.4315 x_{Tc} - 0.3290 x_{Tw} + 0.7338 x_{Kc}) y_{t-1}(\mathbf{x}) + Z_t(\mathbf{x}), \end{aligned}$$

where $\hat{\sigma} = 0.40$, the estimated power exponential correlation parameters are $\hat{\boldsymbol{\theta}} = (\hat{\theta}_{K_{f,p}}, \hat{\theta}_{K_{r,p}}, \hat{\theta}_{T_{half}}, \hat{\theta}_{Tc}, \hat{\theta}_{Tw}, \hat{\theta}_{Kc}) = (1.9065, 0.3041, 1.8212, 0.0202, 2.6826, 0.0210)$.

The forced induction mechanism has five control variables which are the same as the first five in the free induction mechanism (except that x_{Kc} is removed). Similar to the analysis procedure before, the following model can be obtained:

$$\begin{aligned} \text{logit}(p_t(\mathbf{x})) = & -0.6186 + \hat{\varphi}_1 y_{t-1}(\mathbf{x}) + \hat{\alpha}_1 x_{K_{f,p}} + \hat{\alpha}_2 x_{K_{r,p}} + \hat{\alpha}_3 x_{T_{half}} + \hat{\alpha}_4 x_{Tc} + \hat{\alpha}_5 x_{Tw} + \\ & (\hat{\gamma}_1 x_{K_{f,p}} + \hat{\gamma}_2 x_{K_{r,p}} + \hat{\gamma}_3 x_{T_{half}} + \hat{\gamma}_4 x_{Tc} + \hat{\gamma}_5 x_{Tw}) y_{t-1}(\mathbf{x}) + Z_t(\mathbf{x}), \end{aligned}$$

	Standard			
	Value	deviation	Z score	<i>p</i> -value
$\hat{\varphi}_1$	-0.5753	0.0762	-7.5509	0.0000
$\hat{\alpha}_1$	0.2291	0.0427	5.3609	0.0000
$\hat{\alpha}_2$	0.7130	0.0421	16.9521	0.0000
$\hat{\alpha}_3$	0.0337	0.0429	0.7854	0.4322
$\hat{\alpha}_4$	0.9788	0.0419	23.3453	0.0000
$\hat{\alpha}_5$	-0.1363	0.0423	-3.2210	0.0013
$\hat{\alpha}_6$	0.2671	0.0425	6.2847	0.0000
$\hat{\gamma}_1$	0.3183	0.0602	5.2913	0.0000
$\hat{\gamma}_2$	0.4740	0.0602	7.8697	0.0000
$\hat{\gamma}_3$	-0.1903	0.0610	-3.1221	0.0018
$\hat{\gamma}_4$	0.4343	0.0618	7.0301	0.0000
$\hat{\gamma}_5$	-0.3370	0.0616	-5.4669	0.0000
$\hat{\gamma}_6$	0.7412	0.0613	12.0824	0.0000

Table 4: Estimation results for the free induction mechanism.

where all the control variables are standardized into $[0, 1]$, $\hat{\sigma} = 0.33$, the estimated power exponential (with $p = 2$) correlation parameters are $\hat{\boldsymbol{\theta}} = (\hat{\theta}_{K_{f,p}}, \hat{\theta}_{K_{r,p}}, \hat{\theta}_{T_{half}}, \hat{\theta}_{Tc}, \hat{\theta}_{Tw}) = (13.9330, 0.1522, 0.6866, 0.0170, 16.8368)$, and the estimation and inference results for the mean function coefficients are given in Table 5. It can be seen from Table 5 that, with the same significant level, the forced induction mechanism is dominated by only four effects in the mean function, which is a smaller model compared to that for the free induction mechanism. By removing the insignificant effects, the final model can be written as:

$$\text{logit}(p_t(\mathbf{x})) = -0.6125 + 0.1681x_{K_{f,p}} + 0.1039x_{K_{r,p}} + 0.5716x_{Tc} + 0.186x_{K_{r,p}}y_{t-1} + Z_t(\mathbf{x}),$$

where $\hat{\sigma} = 0.34$ and the estimated power exponential correlation parameters are $\hat{\boldsymbol{\theta}} = (\hat{\theta}_{K_{f,p}}, \hat{\theta}_{K_{r,p}}, \hat{\theta}_{T_{half}}, \hat{\theta}_{Tc}, \hat{\theta}_{Tw}) = (1.8208, 0.2033, 0.7712, 0.0173, 8.1983)$.

	Standard			
	Value	deviation	Z score	<i>p</i> -value
$\hat{\varphi}_1$	0.0253	0.0774	0.3268	0.7438
$\hat{\alpha}_1$	0.1629	0.0465	3.5069	0.0005
$\hat{\alpha}_2$	0.1234	0.0434	2.8430	0.0045
$\hat{\alpha}_3$	-0.0138	0.0454	-0.3033	0.7616
$\hat{\alpha}_4$	0.5960	0.0411	14.4836	0.0000
$\hat{\alpha}_5$	-0.0102	0.0447	-0.2290	0.8188
$\hat{\gamma}_1$	-0.0392	0.0700	-0.5595	0.5758
$\hat{\gamma}_2$	0.1756	0.0642	2.7375	0.0062
$\hat{\gamma}_3$	-0.0392	0.0663	-0.5908	0.5546
$\hat{\gamma}_4$	-0.0781	0.0631	-1.2372	0.2160
$\hat{\gamma}_5$	0.1316	0.0667	1.9717	0.0486

Table 5: *Estimation results for the forced induction mechanism.*

By comparing the analyses of the two mechanisms, we see several significant differences, which cannot be directly observed experimentally. The fitted models show that among the interaction effects, all the control variables except $x_{T_{half}}$ are significant for inducing memory in the free induction model, whereas only $x_{Kr,p}$ and x_{Tw} are significant in the force induction model. The application of this statistical approach to the analysis of simulations and experimental data will be powerful in illuminating the unknown biological mechanism, and also informs the next round of experiments by advising future manipulations. Additionally, developments on the calibration of computer experiments based upon the proposed predictive distribution will help provide insight into the range of possible values of variables, such as the increases in kinetic rates, which are difficult to determine through existing methods due to the small time scale at which this mechanism operates and the limits of existing experimental techniques.

6 Summary and Concluding Remarks

In spite of the prevalence of Gaussian process models in the analysis of computer experiments, their applications are limited to the Gaussian assumption on the responses. Motivated by the study of cell adhesion where the computer simulation responses are binary time series, a generalized Gaussian process model is proposed in this paper. The estimation procedure is introduced and asymptotic properties are derived. An optimal predictor and its predictive distribution are constructed which can be used for uncertainty quantification and calibration of future computer simulations. An **R** package is available for implementing the proposed methodology. The methodology is applied to analyze computer simulations of two cell adhesion mechanisms. The results reveal significant differences between the two mechanisms and provide valuable insights on how the next round of lab experiments should be conducted.

The current work can be extended in several directions. First, we will extend the proposed method to other non-Gaussian data, such as the count data. It is conceivable that the current estimation procedure can be directly extended to other exponential family distributions, but different predictive distributions are expected for different types of non-Gaussian data. Second, the computational cost in the proposed procedure can be further reduced. In particular, the inversion of \mathbf{R}_θ can be computationally prohibitive when sample size is large. This computational issue has been addressed for conventional GP models in the recent literature. Extensions of these methods (e.g., Gramacy and Apley (2015); Sung et al. (2017)) to binary responses deserve further attention. Third, many mathematical models underlying the computer simulations contain unknown parameters, which need to be estimated using data from lab experiments. This problem is called calibration and much work has been done in the computer experiment literature. However, the existing methods

(e.g., Kennedy and O'Hagan (2001), Tuo and Wu (2015) and Gramacy et al. (2015)) are only applicable under the Gaussian assumption. Based upon the model and prediction procedure proposed herein, we will work on developing a calibration method for non-Gaussian data.

Appendices

A Assumptions for Proofs

1. The parameter β belongs to an open set $B \subseteq \mathbb{R}^m$.
2. The model matrix X_{it} lies almost surely in a nonrandom compact subset of \mathbb{R}^m such that $Pr(\sum_{i=1}^n \sum_{t=1}^T X'_{it} X_{it} > 0) = 1$.

For any matrix A , define $\|A\| \equiv \sqrt{\text{tr}(A'A)}$; for a covariance matrix $\mathbf{V}(\omega)$, define $V_i(\omega) \equiv \partial \mathbf{V}(\omega) / \partial \omega_i$ and $V_{ij}(\omega) \equiv \partial \mathbf{V}(\omega) / \partial \omega_i \partial \omega_j$; for $\omega \in \Omega$, denote \xrightarrow{u} as uniform convergence of nonrandom functions over compact subsets of Ω .

3. $J_N(\omega)P_N(\omega)^{-1} \xrightarrow{d} W(\omega)$ for some nonsingular $W(\omega)$, which is continuous in ω , where $P_N(\omega) = \text{diag}(\|\Pi(\omega)V_1(\omega)\|, \dots, \|\Pi(\omega)V_{d+1}(\omega)\|)$ and $\Pi(\omega) = \mathbf{V}(\omega)^{-1} - \mathbf{V}(\omega)^{-1}\mathbf{X}(\mathbf{X}'\mathbf{V}(\omega)^{-1}\mathbf{X})^{-1}\mathbf{X}'\mathbf{V}(\omega)^{-1}$.
4. If there exists a sequence $\{r_N\}_{N \geq 1}$ with $1 \leq r_N < N - m$ for all $N \geq 1$, such that

$$(\lambda_N/\lambda_1)^4 \left\{ N/(N - r_N - m)^2 \right\} \left\{ \sum_{i=1}^{d+1} (\lambda_N^i/\lambda_{r_N}^i)^2 \right\}^2 \xrightarrow{u} 0 \quad \text{and}$$

$$(\lambda_N^2/\lambda_1)^2 \left\{ N/(N - r_N - m)^2 \right\}^2 \left\{ \sum_{i=1}^{d+1} \sum_{j=1}^{d+1} (\lambda_N^{ij})^2 (\lambda_N^{ij})^2 (\lambda_{r_N}^i \lambda_{r_N}^j)^{-2} \right\} \xrightarrow{u} 0,$$

where $|\lambda_1| \leq \dots \leq |\lambda_N|$ are the absolute eigenvalues of $\mathbf{V}(\boldsymbol{\omega})$, $|\lambda_1^i| \leq \dots \leq |\lambda_N^i|$ are the absolute eigenvalues of $V_i(\boldsymbol{\omega})$, and $|\lambda_1^{ij}| \leq \dots \leq |\lambda_N^{ij}|$ are the absolute eigenvalues of $V_{ij}(\boldsymbol{\omega})$.

B Proof of Theorem 2.1

The model (3) can be seen as a binary time series model with random effects by multiplying an identity matrix on \mathbf{Z} , that is,

$$\text{logit}(\mathbf{p}) = \mathbf{X}\boldsymbol{\beta} + I_N \mathbf{Z}, \quad \mathbf{Z} \sim \mathcal{N}(\mathbf{0}_N, \Sigma(\boldsymbol{\omega})),$$

where I_N and \mathbf{Z} are viewed as the model matrix and coefficients of random effects, respectively. Therefore, if the variance-covariance parameters are given, the inference of $\boldsymbol{\beta}$ is a special case of the binary time series model with random effects in Hung et al. (2008). Therefore, following Theroem 1 in Hung et al. (2008), the score function $S_N(\boldsymbol{\beta}, \boldsymbol{\omega})$ is asymptotically normally distributed.

C Proof of Theorem 2.2

According to Breslow and Clayton (1993), one can view the inference on the variance-variance component as an iterative procedure for the linear mixed model

$$\tilde{\boldsymbol{\eta}} = \mathbf{X}\boldsymbol{\beta} + I_N \mathbf{Z} + \boldsymbol{\epsilon}, \quad \boldsymbol{\epsilon} \sim \mathcal{N}(\mathbf{0}_N, \mathbf{W}^{-1})$$

with the iterative weight \mathbf{W}^{-1} . Thus, it is a special case of the Gaussian general linear model in Cressie and Lahiri (1993) with response vector $\tilde{\boldsymbol{\eta}}$ and variance-covariance component

$\Sigma(\boldsymbol{\omega}) + \mathbf{W}^{-1}$ with parameters $\boldsymbol{\omega}$. Since the asymptotic distribution of REML estimators for the variance-covariance parameters has been shown in Cressie and Lahiri (1993) for a Gaussian general linear model, the result directly follows as a special case of Corollary 3.3 in Cressie and Lahiri (1993).

D Proof of Lemma 3.1

We start the proof by deriving the conditional distribution from a simple model (2) (without time-series), and then extend the result to prove Lemma 3.1. First, a definition and a lemma about multivariate log-normal distribution are in order.

Definition D.1. Suppose $\boldsymbol{\xi} = (\xi_1, \dots, \xi_n)'$ has a multivariate normal distribution with mean $\boldsymbol{\mu}_n$ and covariance variance $\boldsymbol{\Sigma}_{n \times n}$. Then $\mathbf{b} = \exp\{\boldsymbol{\xi}\}$ has a *multivariate log-normal distribution*. Denote it as $\mathbf{b} \sim \mathcal{LN}(\boldsymbol{\mu}_n, \boldsymbol{\Sigma}_{n \times n})$.

Lemma D.1. Suppose \mathbf{b}^n and b_{n+1} have a multivariate log-normal distribution

$$\begin{pmatrix} \mathbf{b}^n \\ b_{n+1} \end{pmatrix} \sim \mathcal{LN} \left(\begin{pmatrix} \boldsymbol{\mu}^n \\ \mu_{n+1} \end{pmatrix}, \begin{bmatrix} \boldsymbol{\Sigma}_{n \times n} & \mathbf{r} \\ \mathbf{r}' & \sigma_{n+1}^2 \end{bmatrix} \right).$$

The conditional distribution of b_{n+1} given \mathbf{b}^n is $b_{n+1} | \mathbf{b}^n \sim \mathcal{LN}(\mu^*, v^*)$, where $\mu^* = \mu_{n+1} + \mathbf{r}' \boldsymbol{\Sigma}_{n \times n}^{-1} (\log \mathbf{b}^n - \boldsymbol{\mu}^n)$ and $v^* = \sigma_{n+1}^2 - \mathbf{r}' \boldsymbol{\Sigma}_{n \times n}^{-1} \mathbf{r}$.

Proof. Using transformation of a standard normal distribution, one can show that the joint probability density function of the multivariate log-normal distribution \mathbf{b}^n is

$$g_{\mathbf{b}^n}(b_1, \dots, b_n) = \frac{1}{(2\pi)^{n/2} |\boldsymbol{\Sigma}_{n \times n}|^{1/2}} \frac{1}{\prod_{i=1}^n b_i} \exp\left\{-\frac{1}{2} (\log \mathbf{b}^n - \boldsymbol{\mu}_n)' \boldsymbol{\Sigma}_{n \times n}^{-1} (\log \mathbf{b}^n - \boldsymbol{\mu}_n)\right\}.$$

Denote $\mathbf{b}^{n+1} = (b_1, \dots, b_n, b_{n+1})$, $\boldsymbol{\mu}^{n+1} = (\mu_1, \dots, \mu_n, \mu_{n+1})$ and

$$\boldsymbol{\Sigma}_{(n+1) \times (n+1)} = \begin{bmatrix} \boldsymbol{\Sigma}_{n \times n} & \mathbf{r} \\ \mathbf{r}' & \sigma_{n+1} \end{bmatrix}.$$

Then, the conditional probability density function of b_{n+1} given \mathbf{b}^n can be derived as

$$\begin{aligned} g_{b_{n+1}|\mathbf{b}^n}(b_{n+1}|\mathbf{b}^n) &\propto g(b_1, \dots, b_n, b_{n+1}) \\ &\propto \frac{1}{b_{n+1}} \exp\left\{-\frac{1}{2} (\log \mathbf{b}^{n+1} - \boldsymbol{\mu}_{n+1})' \boldsymbol{\Sigma}_{(n+1) \times (n+1)}^{-1} (\log \mathbf{b}^{n+1} - \boldsymbol{\mu}_{n+1})\right\}. \end{aligned}$$

Let $\mathbf{a}_1 = \log \mathbf{b}^n - \boldsymbol{\mu}^n$ and $\mathbf{a}_2 = \log \mathbf{b}^{n+1} - \boldsymbol{\mu}^{n+1}$. Applying the partitioned matrix inverse results (page 99 of Harville (1997)) gives

$$\begin{aligned} &(\log \mathbf{b}^{n+1} - \boldsymbol{\mu}^{n+1})' \boldsymbol{\Sigma}_{(n+1) \times (n+1)}^{-1} (\log \mathbf{b}^{n+1} - \boldsymbol{\mu}^{n+1}) \\ &= \begin{bmatrix} \mathbf{a}'_1 & \mathbf{a}'_2 \end{bmatrix} \begin{bmatrix} \boldsymbol{\Sigma}_{n \times n} & \mathbf{r} \\ \mathbf{r}' & \sigma_{n+1} \end{bmatrix}^{-1} \begin{bmatrix} \mathbf{a}_1 \\ \mathbf{a}_2 \end{bmatrix} \\ &= (\mathbf{a}_2 - \mathbf{r}' \boldsymbol{\Sigma}_{n \times n}^{-1} \mathbf{a}_1)' \sigma_{22 \cdot 1}^{-1} (\mathbf{a}_2 - \mathbf{r}' \boldsymbol{\Sigma}_{n \times n}^{-1} \mathbf{a}_1) + \mathbf{a}'_1 \boldsymbol{\Sigma}_{n \times n}^{-1} \mathbf{a}_1 \\ &= (\mathbf{a}_2 - \mathbf{r}' \boldsymbol{\Sigma}_{n \times n}^{-1} \mathbf{a}_1)^2 / \sigma_{22 \cdot 1} + \mathbf{a}'_1 \boldsymbol{\Sigma}_{n \times n}^{-1} \mathbf{a}_1, \end{aligned}$$

where $\sigma_{22 \cdot 1} = \sigma_{n+1}^2 - \mathbf{r}' \boldsymbol{\Sigma}_{n \times n}^{-1} \mathbf{r}$ and is a real number.

Thus, the conditional probability density function of b_{n+1} given \mathbf{b}^n can be simplified to

$$\begin{aligned} g_{b_{n+1}|\mathbf{b}^n}(b_{n+1}|\mathbf{b}^n) &\propto \frac{1}{b_{n+1}} \exp\left\{-\frac{1}{2\sigma_{22.1}}(\mathbf{a}_2 - \mathbf{r}'\Sigma_{n\times n}^{-1}\mathbf{a}_1)^2 - \frac{1}{2}\mathbf{a}_1'\Sigma_{n\times n}^{-1}\mathbf{a}_1\right\} \\ &\propto \frac{1}{b_{n+1}} \exp\left\{-\frac{1}{2\sigma_{22.1}}(\mathbf{a}_2 - \mathbf{r}'\Sigma_{n\times n}^{-1}\mathbf{a}_1)^2\right\} \\ &= \frac{1}{b_{n+1}} \exp\left\{-\frac{1}{2\sigma_{22.1}}\left(\log b_{n+1} - (\mu_{n+1} + \mathbf{r}'\Sigma_{n\times n}^{-1}(\log \mathbf{b}^n - \boldsymbol{\mu}^n))\right)^2\right\}. \end{aligned}$$

Therefore, according to the probability density function of a log-normal distribution, we have $b_{n+1}|\mathbf{b}^n \sim \mathcal{LN}(\mu^*, v^*)$, where $\mu^* = \mu_{n+1} + \mathbf{r}'\Sigma_{n\times n}^{-1}(\log \mathbf{b}^n - \boldsymbol{\mu}^n)$ and $v^* = \sigma_{22.1}^2 = \sigma_{n+1}^2 - \mathbf{r}'\Sigma_{n\times n}^{-1}\mathbf{r}$. \square

Lemma D.2. *Consider the model (2) (without time-series), given $(p(\mathbf{x}_1), \dots, p(\mathbf{x}_n))' = \mathbf{p}^n$, the conditional distribution of $p(\mathbf{x}_{n+1})$ is a logit-normal distribution, that is, $p(\mathbf{x}_{n+1})|\mathbf{p}^n \sim \text{Logitnormal}(m(\mathbf{p}^n), v(\mathbf{p}^n))$ with $m(\mathbf{p}^n) = \mu(\mathbf{x}_{n+1}) + \mathbf{r}'\mathbf{R}_{\boldsymbol{\theta}}^{-1}(\log \frac{\mathbf{p}^n}{1-\mathbf{p}^n} - \boldsymbol{\mu}^n)$ and $v(\mathbf{p}^n) = \sigma^2(1 - \mathbf{r}'\mathbf{R}_{\boldsymbol{\theta}}^{-1}\mathbf{r}_{\boldsymbol{\theta}})$, where $\boldsymbol{\mu}^n = (\mu(\mathbf{x}_1), \dots, \mu(\mathbf{x}_n))'$, $\mathbf{r}_{\boldsymbol{\theta}} = (R_{\boldsymbol{\theta}}(\mathbf{x}_{n+1}, \mathbf{x}_1), \dots, R_{\boldsymbol{\theta}}(\mathbf{x}_{n+1}, \mathbf{x}_n))'$, and $\mathbf{R}_{\boldsymbol{\theta}} = \{R_{\boldsymbol{\theta}}(\mathbf{x}_i, \mathbf{x}_j)\}$.*

Proof. Let $\eta_i = \mu(\mathbf{x}_i) + Z(\mathbf{x}_i)$ and $b_i = \exp\{\eta_i\} = p(\mathbf{x}_i)/(1 - p(\mathbf{x}_i))$ for $i = 1, \dots, n+1$. Since $(\eta_1, \dots, \eta_n, \eta_{n+1})' \sim \mathcal{N}(\boldsymbol{\mu}^{n+1}, \sigma^2 \mathbf{R}_{\boldsymbol{\theta}}^*)$, where $\boldsymbol{\mu}^{n+1} = ((\boldsymbol{\mu}^n)', \mu(\mathbf{x}_{n+1}))'$ and

$$\mathbf{R}_{\boldsymbol{\theta}}^* = \begin{bmatrix} \mathbf{R}_{\boldsymbol{\theta}} & \mathbf{r}_{\boldsymbol{\theta}} \\ \mathbf{r}'_{\boldsymbol{\theta}} & 1 \end{bmatrix},$$

we have $(b_1, \dots, b_n, b_{n+1})' \sim \mathcal{LN}(\boldsymbol{\mu}^{n+1}, \sigma^2 \mathbf{R}_{\boldsymbol{\theta}}^*)$ by Definition D.1. Thus, using Jacobian of

the transformation and Lemma D.1, we have

$$\begin{aligned}
& g_{p(\mathbf{x}_{n+1})|p(\mathbf{x}_1), \dots, p(\mathbf{x}_n)}(p_{n+1}|p_1, \dots, p_n) \\
&= g_{b_{n+1}|b_1, \dots, b_n}(\frac{p_{n+1}}{1-p_{n+1}} | \frac{p_1}{1-p_1}, \dots, \frac{p_n}{1-p_n}) \frac{1}{(1-p_{n+1})^2} \\
&\propto \frac{1-p_{n+1}}{p_{n+1}} \exp\left\{-\frac{\left(\log \frac{p_{n+1}}{1-p_{n+1}} - (\mu(\mathbf{x}_{n+1}) + \mathbf{r}'_{\theta} \mathbf{R}_{\theta}^{-1} (\log \frac{\mathbf{p}^n}{1-\mathbf{p}^n} - \boldsymbol{\mu}^n))\right)^2}{2\sigma^2(1 - \mathbf{r}'_{\theta} \mathbf{R}_{\theta}^{-1} \mathbf{r}_{\theta})}\right\} \frac{1}{(1-p_{n+1})^2} \\
&\propto \frac{1}{p_{n+1}(1-p_{n+1})} \exp\left\{-\frac{\left(\log \frac{p_{n+1}}{1-p_{n+1}} - (\mu(\mathbf{x}_{n+1}) + \mathbf{r}'_{\theta} \mathbf{R}_{\theta}^{-1} (\log \frac{\mathbf{p}^n}{1-\mathbf{p}^n} - \boldsymbol{\mu}^n))\right)^2}{2\sigma^2(1 - \mathbf{r}'_{\theta} \mathbf{R}_{\theta}^{-1} \mathbf{r}_{\theta})}\right\}.
\end{aligned}$$

Therefore, according to the probability density function of a logit-normal distribution, we have $p(\mathbf{x}_{n+1})|\mathbf{p}^n \sim \text{Logitnormal}(m(\mathbf{p}^n), v(\mathbf{p}^n))$. \square

Similarly, the result of Lemma D.2 can be extended to the general model (1). Given $\mathbf{Y} = (\mathbf{y}'_1, \dots, \mathbf{y}'_T, y_{n+1,1}, \dots, y_{n+1,s-1})'$, at a fixed time-step s , $p_s(\mathbf{x}_1), \dots, p_s(\mathbf{x}_n), p_s(\mathbf{x}_{n+1})$ can be seen to have the model (2) with mean function $\mu(\mathbf{x}_i, \mathbf{Y}) = \sum_{r=1}^R \varphi_r y_{i,s-r} + \mathbf{x}'_i \boldsymbol{\alpha} + \sum_{l=1}^L \gamma_l \mathbf{x}_i y_{i,s-l}$. Thus, by Lemma D.2, denote $\mathbf{p}_s = (p_s(\mathbf{x}_1), \dots, p_s(\mathbf{x}_n))'$, we have

$$p_s(\mathbf{x}_{n+1})|\mathbf{p}_s, \mathbf{Y} \sim \text{Logitnormal}(m(\mathbf{p}_s, \mathbf{Y}), v(\mathbf{p}_s, \mathbf{Y})),$$

where $m(\mathbf{p}_s, \mathbf{Y}) = \mu(\mathbf{x}_{n+1}, \mathbf{Y}) + \mathbf{r}'_{\theta} \mathbf{R}_{\theta}^{-1} (\log \frac{\mathbf{p}_s}{1-\mathbf{p}_s} - \boldsymbol{\mu}^n)$, $\boldsymbol{\mu}^n = (\mu(\mathbf{x}_1, \mathbf{Y}), \dots, \mu(\mathbf{x}_n, \mathbf{Y}))'$, and $v(\mathbf{p}_s, \mathbf{Y}) = \sigma^2(1 - \mathbf{r}'_{\theta} \mathbf{R}_{\theta}^{-1} \mathbf{r}_{\theta})$. By the fact that $Z_t(\mathbf{x})$ is independent over time, which implies $p_s(\mathbf{x})$ is independent of $p_t(\mathbf{x})$ for any $t \neq s$, $p_s(\mathbf{x}_{n+1})|D_{n+1,s}$ and $p_s(\mathbf{x}_{n+1})|\mathbf{p}_s, \mathbf{Y}$ have the same distribution. So, $p_s(\mathbf{x}_{n+1})|D_{n+1,s} \sim \text{Logitnormal}(m(D_{n+1,s}), v(D_{n+1,s}))$, where $m(D_{n+1,s}) = m(\mathbf{p}_s, \mathbf{Y})$ and $v(D_{n+1,s}) = v(\mathbf{p}_s, \mathbf{Y})$.

E Proof of Theorem 3.2

(i) First, one can show that if $(p_s(\mathbf{x}_{n+1}), D_{n+1,s})$ has a joint distribution for which the conditional mean of $p_s(\mathbf{x}_{n+1})$ given $D_{n+1,s}$ exists, then $\mathbb{E}[p(\mathbf{x}_{n+1})|D_{n+1,s}]$ is the minimum mean squared error predictor of $p(\mathbf{x}_{n+1})$. See Theorem 3.2.1 in Santner et al. (2003). Thus, by the result of Lemma 3.1, we have the conditional mean $\mathbb{E}[p(\mathbf{x}_{n+1})|D_{n+1,s}] = \kappa(m(D_{n+1,s}), v(D_{n+1,s}))$ with variance $\mathbb{V}[p(\mathbf{x}_{n+1})|D_{n+1,s}] = \tau(m(D_{n+1,s}), v(D_{n+1,s}))$.

(ii) If $\mathbf{x}_{n+1} = \mathbf{x}_i$ for $i = 1, \dots, n$, then $m(D_{n+1,s}) = \log(p_s(\mathbf{x}_i)/(1-p_s(\mathbf{x}_i)))$ and $v(D_{n+1,s}) = 0$, which implies that

$$\kappa(m(D_{n+1,s}), 0) = \exp\{m(D_{n+1,s})\}/(1 + \exp\{m(D_{n+1,s})\}) = p_s(\mathbf{x}_i)$$

and $\tau(m(D_{n+1,s}), 0) = 0$ by using transformation of a normal distribution. Thus, by Theorem 3.2 (i), we have $\mathbb{E}[p_s(\mathbf{x}_{n+1})|D_{n+1,s}] = p_s(\mathbf{x}_i)$ and $\mathbb{V}[p_s(\mathbf{x}_{n+1})|D_{n+1,s}] = 0$.

(iii) Let $X \sim \mathcal{N}(m(D_{n+1,s}), v(D_{n+1,s}))$, $P = \exp\{X\}/(1 + \exp\{X\})$, which has the distribution *Logitnormal*($m(D_{n+1,s}), v(D_{n+1,s})$), and $Q(q; D_{n+1,s})$ be the q -th quantile of P . Consider the function $f(x) = \log(x/(1-x))$. The derivative is $f'(x) = 1/(x(1-x))$. Thus, for $0 < x < 1$ the derivative is positive and the $f(x)$ function is increasing in x . Then,

$$\begin{aligned} & \Pr\{P > Q(q; D_{n+1,s})\} = q \\ \Leftrightarrow & \Pr\left\{\frac{\exp\{X\}}{1 + \exp\{X\}} > Q(q; D_{n+1,s})\right\} = q \\ \Leftrightarrow & \Pr\left\{f\left(\frac{\exp\{X\}}{1 + \exp\{X\}}\right) > f(Q(q; D_{n+1,s}))\right\} = q \\ \Leftrightarrow & \Pr\left\{X > \log \frac{Q(q; D_{n+1,s})}{1 - Q(q; D_{n+1,s})}\right\} = q \end{aligned}$$

$$\begin{aligned}
&\Leftrightarrow \Pr \left\{ \frac{X - m(D_{n+1,s})}{\sqrt{v(D_{n+1,s})}} > \frac{1}{\sqrt{v(D_{n+1,s})}} \left(\log \frac{Q(q; D_{n+1,s})}{1 - Q(q; D_{n+1,s})} - m(D_{n+1,s}) \right) \right\} = q \\
&\Leftrightarrow \frac{1}{\sqrt{v(D_{n+1,s})}} \left(\log \frac{Q(q; D_{n+1,s})}{1 - Q(q; D_{n+1,s})} - m(D_{n+1,s}) \right) = z_q \\
&\Leftrightarrow Q(q; D_{n+1,s}) = \frac{\exp\{m(D_{n+1,s}) + z_q \sqrt{v(D_{n+1,s})}\}}{1 + \exp\{m(D_{n+1,s}) + z_q \sqrt{v(D_{n+1,s})}\}}.
\end{aligned}$$

F Algorithm: Metropolis-Hastings Algorithm

```

1: for  $j = 1$  to  $J$  do
2:   Set  $N_s = nT + s - 1$ .
3:   Start with a zero vector  $\mathbf{p}$  of size  $N_s$ .
4:   for  $k = 1$  to  $N_s$  do
5:     Generate a random value  $p_k^*$  from  $\text{Logitnormal}(m(\mathbf{p}_{-k}, \mathbf{y}_{-k}), v(\mathbf{p}_{-k}, \mathbf{y}_{-k}))$ .
6:     Generate an uniform random variable  $U \sim \text{Unif}(0, 1)$ .
7:     if  $U < \min\{1, \frac{f(y_k|p_k^*)}{f(y_k|p_k)}\}$  then
8:       Set  $\mathbf{p} = (p_1, \dots, p_k^*, \dots, p_{N_s})$ .
9:   Set  $\mathbf{p}^{(j)} = \mathbf{p}$ 
10:  Return  $\{\mathbf{p}^{(j)}\}_{j=1, \dots, J}$ .

```

G Algorithm: Dynamic Binary Emulator

```

1: for  $j = 1$  to  $J$  do
2:   Set  $N = nT$ .
3:   Start with a zero vector  $\mathbf{p}$  of size  $N$ .
4:   for  $i = 1$  to  $N$  do

```

```

5: Generate a random value  $p_k^*$  from  $Logitnormal(m(\mathbf{p}_{-k}, \mathbf{y}_{-k}), v(\mathbf{p}_{-k}, \mathbf{y}_{-k}))$ .
6: Generate an uniform random variable  $U \sim Unif(0, 1)$ .
7: if  $U < \min\{1, \frac{f(y_k|p_k^*)}{f(y_k|p_k)}\}$  then
8:   Set  $\mathbf{p} = (p_1, \dots, p_k^*, \dots, p_N)$ .
9: Set  $\mathbf{p}_{n+1} = \mathbf{p}$ ,  $\mathbf{Y}_{n+1} = \mathbf{Y}$ , and a zero vector  $\mathbf{p}_{\text{new}}$  of size  $T$ .
10: for  $t = 1$  to  $T$  do
11:   Given  $D_{n+1,t} = \{\mathbf{p}_{n+1}, \mathbf{Y}_{n+1}\}$ , draw a sample  $p_t(\mathbf{x}_{n+1})$  from  $Logitnormal(m(D_{n+1,t}), v(D_{n+1,t}))$ ,
    and then draw a sample  $y_t(\mathbf{x}_{n+1})$  from a Bernoulli distribution with parameter  $p_t(\mathbf{x}_{n+1})$ .
12:   Update  $\mathbf{p}_{n+1} = (\mathbf{p}'_{n+1}, p_t(\mathbf{x}_{n+1}))'$ ,  $\mathbf{Y}_{n+1} = (\mathbf{Y}'_{n+1}, y_t(\mathbf{x}_{n+1}))'$ , and  $(\mathbf{p}_{\text{new}})_t =$ 
     $p_t(\mathbf{x}_{n+1})$ .
13:   Set  $\mathbf{p}_{\text{new}}^{(j)} = \mathbf{p}_{\text{new}}$ 
14: Take pointwise median from  $\{\mathbf{p}_{\text{new}}^{(j)}\}_{j=1, \dots, J}$ .

```

References

Atchison, J. and Shen, S. M. (1980). Logistic-normal distributions: some properties and uses. *Biometrika*, 67(2):261–272.

Barndorff-Nielsen, O. E. and Cox, D. R. (1997). *Asymptotic Techniques for Use in Statistics*. London: Chapman & Hall.

Breslow, N. E. and Clayton, D. G. (1993). Approximate inference in generalized linear mixed models. *Journal of the American statistical Association*, 88(421):9–25.

Cox, D. R. (1972). Regression models and life-tables. *Journal of the Royal Statistical Society, Series B*, 34(2):187–220.

Cox, D. R. (1975). Partial likelihood. *Biometrika*, 62(2):269–276.

Cressie, N. and Lahiri, S. N. (1993). The asymptotic distribution of reml estimators. *Journal of Multivariate Analysis*, 45(2):217–233.

Cressie, N. and Lahiri, S. N. (1996). Asymptotics for reml estimation of spatial covariance parameters. *Journal of Statistical Planning and Inference*, 50(3):327–341.

Frederic, P. and Lad, F. (2008). Two moments of the logitnormal distribution. *Communications in Statistics Simulation and Computation*, 37(7):1263–1269.

Gramacy, R. B. and Apley, D. W. (2015). Local gaussian process approximation for large computer experiments. *Journal of Computational and Graphical Statistics*, 24(2):561–578.

Gramacy, R. B., Bingham, D., Holloway, J. P., Grosskopf, M. J., Kuranz, C. C., Rutter, E., Trantham, M., and Drake, R. P. (2015). Calibrating a large computer experiment simulating radiative shock hydrodynamics. *The Annals of Applied Statistics*, 9(3):1141–1168.

Harville, D. A. (1974). Bayesian inference for variance components using only error contrasts. *Biometrika*, 61(2):383–385.

Harville, D. A. (1977). Maximum likelihood approaches to variance component estimation and to related problems. *Journal of the American Statistical Association*, 72(358):320–338.

Harville, D. A. (1997). *Matrix Algebra from a Statistician’s Perspective*, volume 157. Springer.

Huang, J., Zarnitsyna, V. I., Liu, B., Edwards, L. J., Jiang, N., Evavold, B. D., and Zhu, C. (2010). The kinetics of two-dimensional tcr and pmhc interactions determine t-cell responsiveness. *Nature*, 464(7290):932–936.

Hung, Y., Zarnitsyna, V., Zhang, Y., Zhu, C., and Wu, C. F. J. (2008). Binary time series modeling with application to adhesion frequency experiments. *Journal of the American Statistical Association*, 103(483).

Kennedy, M. C. and O'Hagan, A. (2001). Bayesian calibration of computer models (with discussion). *Journal of the Royal Statistical Society: Series B*, 63(3):425–464.

Li, R. and Sudjianto, A. (2005). Analysis of computer experiments using penalized likelihood in gaussian kriging models. *Technometrics*, 47(2):111–120.

Liu, F. and West, M. (2009). A dynamic modelling strategy for bayesian computer model emulation. *Bayesian Analysis*, 4(2):393–411.

Mead, R. (1965). A generalised logit-normal distribution. *Biometrics*, 21(3):721–732.

Patterson, H. D. and Thompson, R. (1971). Recovery of inter-block information when block sizes are unequal. *Biometrika*, 58(3):545–554.

Patterson, H. D. and Thompson, R. (1974). Maximum likelihood estimation of components of variance. In *Proceedings of the 8th International Biometric Conference*, pages 197–207. Biometric Society, Washington, DC.

R Core Team (2015). *R: A Language and Environment for Statistical Computing*. R Foundation for Statistical Computing, Vienna, Austria.

Rasmussen, C. E. and Williams, C. K. I. (2006). *Gaussian Processes for Machine Learning*. the MIT Press.

Sacks, J., Welch, W. J., Mitchell, T. J., and Wynn, H. P. (1989). Design and analysis of computer experiments. *Statistical Scicence*, 4(4):409–423.

Santner, T. J., Williams, B. J., and Notz, W. I. (2003). *The Design and Analysis of Computer Experiments*. Springer New York.

Slud, E. and Kedem, B. (1994). Partial likelihood analysis of logistic regression and autoregression. *Statistica Sinica*, 4(1):89–106.

Sung, C.-L. (2017). *binaryGP: fit and predict a Gaussian process model with (time-series) binary response*. R package version 0.1.

Sung, C.-L., Gramacy, R. B., and Haaland, B. (2017). Potentially predictive variance reducing subsample locations in local gaussian process regression. *Statistica Sinica*, to appear. arXiv preprint arXiv:1604.04980.

Tang, B. (1993). Orthogonal array-based latin hypercubes. *Journal of the American Statistical Association*, 88(424):1392–1397.

Tuo, R. and Wu, C. F. J. (2015). Efficient calibration for imperfect computer models. *Annals of Statistics*, 43(6):2331–2352.

Wutzler, T. (2012). *logitnorm: Functions for the logitnormal distribution*. R package version 0.8.29.

Zarnitsyna, V. I., Huang, J., Zhang, F., Chien, Y.-H., Leckband, D., and Zhu, C. (2007). Memory in receptor-ligand-mediated cell adhesion. *Proceedings of the National Academy of Science, U.S.A.*, 104(46):18037–18042.

Zeger, S. L. and Qaqish, B. (1988). Markov regression models for time series: a quasi-likelihood approach. *Biometrics*, 44(4):1019–1031.

Zhang, H. (2002). On estimation and prediction for spatial generalized linear mixed models. *Biometrics*, 58(1):129–136.